15 MHz Single Element Ultrasound Needle Transducers for Neurosurgical Applications

Yun Jiang, Carl Meggs, Tim Button
University of Birmingham
Birmingham, UK
t.w.button@bham.ac.uk

Giuseppe Schiavone, Marc P.Y. Desmulliez
Heriot-Watt University
Edinburgh, UK
m.desmulliez@hw.ac.uk

Zhen Qiu, Syed Mahboob, Rachael McPhillips, Christine E.M Démoré, Graeme Casey, Sam Eljamel, Sandy Cochran
University of Dundee
Dundee, UK
s.cochran@dundee.ac.uk

Daniel Rodriguez Sanmartin
Applied Functional Materials Ltd.
Birmingham, UK
daniel.sanmartin@afm-ltd.com

***Abstract*—Image-guided surgery is today considered to be of significant importance in neurosurgical applications. However, one of its major shortcomings is its reliance on preoperative image data, which does not account for the intraoperative brain deformations and displacements that occur during surgery. In this work, we propose to tackle this issue with the incorporation of an ultrasound device within a biopsy needle that is commonly used as an interventional tool so as to provide immediate feedback to neurosurgeons during surgical procedures. In order to identify the most appropriate path to access a targeted tissue site, needle single element transducers that look both forwards and sideways have been designed and fabricated. Monolithic PZT plates and micro-moulded 1-3 piezocomposites have been adopted as the active materials for feasibility tests. Impedance analysis and pulse-echo testing have been carried out, demonstrating the functionality of the transducers at frequencies of ~15 MHz. The imaging capabilities of these transducers have been studied by wire phantom scans. Variations in the transducer properties as a result of the use of different active materials are discussed.**

Keywords—1-3 composite; needle ultrasound transducer; neurosurgery

I. INTRODUCTION

Neurosurgical intervention is required for a broad range of diseases and disorders such as brain tumours and intercranial haematomas. Localisation of the intracranial target has for decades predominately relied on preoperative images acquired from computed tomography (CT) and magnetic resonance imaging (MRI) [1,2]. In conventionally used procedures, the accurate coordinates of the target are identified from the preoperative images and then a stereotactic frame is applied to navigate an interventional tool such as a biopsy needle based on the acquired coordinates. However, shifting and deformation of the brain tissues occur in the course of the surgery in response to a variety of physical and physiological phenomena in the opened skull, including head-position alteration, raised intracranial pressure and cerebrospinal fluid drainage [3], and therefore preoperative image-guided navigation can become inaccurate and unreliable. Maximum brain shifts of more than 20 mm have been reported [4,5]. Such significant inaccuracies between a calculated target location and its actual position during surgery could potentially have an adverse effect on a patient's post-operative recovery as well as the effectiveness of the neurosurgical procedure.

Determination of brain shifts by mathematic models has also proven to be rather difficult [6]. Intraoperative image-guided navigation has therefore gained growing interest as a reliable alternative to preoperative image guided navigation techniques. Both intraoperative CT and MRI have demonstrated their usefulness in neurosurgical applications [7,8], however, these systems suffer from several intrinsic disadvantages including interruption of the workflow during the intervention, difficult positioning of the patient, limited access for the surgeon to the operative field, as well as high cost. In comparison, intraoperative ultrasound (IOS) has recently attracted increasing interest not only because of its well-acknowledged safety, portability and low cost but also, and more importantly, due to its real-time visualisation capability and its improved image quality [5]. However, one of the biggest limitations of the existing IOS technology lies in the requirement for an undesirably large craniotomy, as a relatively large aperture probe is needed for imaging deep brain structures [9].

In this work, we propose the use of a biopsy needle that is capable of minimally invasive and high-resolution ultrasound imaging to overcome the drawback of current IOS systems. The incorporation of single element transducers looking forward and sideways within a needle would enable the neurosurgeon to obtain intraoperative real-time image-guided

The work reported here has been supported by the Engineering and Physical Research Council, UK.

information about the intricate brain structures that lie in the path of the needle on the way to the target site of interest.

Commercial monolithic lead zirconate titanate (PZT) elements were used as the active materials for initial feasibility tests, followed by the use of 1-3 piezocomposites that have been widely perceived as the preferred active material for medical ultrasound transducers. As an alternative to conventional dice-and-fill methods, a micro-moulding approach combining viscous polymer processing (VPP) and lost polymer mould techniques has been applied for the fabrication of the piezocomposites used in these single element devices. The operational frequency for the transducers was designed to be 15 MHz, as this work represents the first step towards array needle transducers whose fully operational frequencies are limited at around 20 MHz by electronic systems.

II. Fabrication Methods

A. PZT octagons

Commercial CTS 3203HD grade PZT plates (CTS Corp., UK) supplied in a poled condition were diced into octagons to suit the inner diameter (ID) of the needles using a MicroAce 66 Dicing Machine (Loadpoint Ltd., UK). The major dimensions of the octagons (distance across opposite corners and faces) were 1.768 and 1.633 mm respectively, and the plates were 0.148 mm thick. Electroding was carried out using a Peltier cooled sputter coater (Emitech K575, Emitech Ltd., UK), in which a thin layer (~10 nm) of Cr and a thicker layer (~200 nm) of Au were deposited sequentially on both sides of the octagons. The transducers incorporating these octagons facing forwards and sideways are named Trdx-FF1 and Trdx-SF1, respectively.

B. 1-3 Piezocomposites

VPP-based fabrication of 1-3 piezocomposites involved the following processing stages. Firstly, a sheet of PZT based dough was obtained from high shear milling of a commercial PZT-5H type powder (TRS610C, TRS Ceramics, USA, with a primary particle size of 1.2 μm), distilled water, Polyvinyl alcohol-acetate binder (KH-1075, Nippon Synthetic Chemical Industry Co. Ltd, Japan) and other additives by a twin roll mill (Winkworth Machinery, UK). Secondly, a disc with a diameter of 13 mm was cut from the VPP sheet to fit the size of a uniaxial die, followed by an embossing stage where the VPP material was pressed into a polycarbonate mould using a Instron 5507 mechanical testing machine (Instron, UK). Thirdly, the mould was dissolved in an organic solvent after drying the green discs using a three-step drying regime. The resulting bristle-block structure was buried in lead oxide doped zirconia sand to compensate for any lead loss during sintering and sintered at 1200°C for 1 h. The sintered sample was then encapsulated with Epofix epoxy (Struers, UK) and lapped using a PM5 precision lapping machine (Logitech, UK) to the required thickness for 15 MHz operation.

Fig. 1 shows an optical micrograph of a VPP composite, in which the pillars with a diameter of ~20 μm and a kerf of ~8 μm are arranged hexagonally.

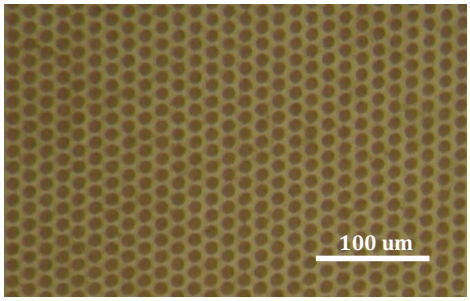

Fig. 1. Optical image of a VPP composite (top View), where the darker areas are the pillars and the lighter area is the polymer matrix.

Poling of the composites was carried out in a bespoke corona poling jig at 120°C for 10 min with a voltage of 30 kV before depositing chrome-gold electrodes on both sides of the composite area as described for the PZT octagons. The composites were then laser-cut into discs with a diameter of 1.7 mm, ready for the transducer fabrication. The transducers incorporating these composites facing forwards and sideways are named Trdx-FF1 and Trdx-SF1, respectively.

C. Single element needle transducers

During the development of the needle transducers, the outer cannula of a stainless steel brain biopsy needle (Pajunk, UK) with length, inner diameter (ID) and outer diameter (OD) dimensions of 80 mm, 1.8 mm and 2.3 mm respectively, and with a lateral opening of 3 mm was initially selected to be the casing for transducer Trdx-SF1. However, as later characterisation was to include the use of MRI, non-magnetic and similarly sized brass tubes (Speciality Metals, UK) with corresponding dimensions of 80 mm, 1.8 mm and 2.4 mm respectively were used for the other three transducers, of which the one for Trdx-SF2 had a lateral opening of 3 mm.

For the forward-facing transducers, an enameled copper wire with a diameter of 80 μm was connected onto one of the electrodes of the active material with silver epoxy (RS, UK) followed by a cast-in-place fabrication process of a tungsten epoxy backing. After curing at room temperature, the whole assembly was inserted into the case and an MCX connector was soldered onto the wire and then glued into the end of the needle.

For the side-facing transducers, a tungsten epoxy insert made to fit the lateral opening of the needle was fabricated. A hole of approximately 300 μm diameter was drilled through the insert to provide an access point for the copper wire to be connected to the bottom electrode. The composite was then mounted to the insert before fitting the completed insert into the needle.

Fig. 2 shows a photograph of a set of the assembled needle transducers, one orientated forwards and one sideways, together with close-up images of the PZT octagons and composites mounted on the needles.

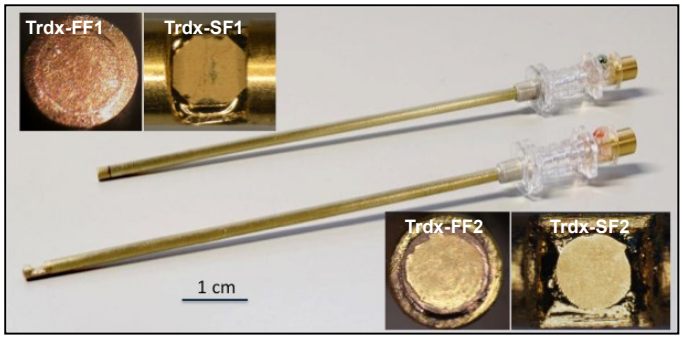

Fig. 2. Photographs of single element needle transducers. The four inset images show close-up pictures of the front-facing (Trdx-FF1 and Trdx-FF2) and the side-facing (Trdx-SF1 and Trdx-SF2) tranducers.

III. Transducer Characterisation

A. Impedance analysis

The electrical impedance spectra of the four assembled needle transducers were measured by a precision impedance analyser (4395A, Agilent Technologies UK Ltd., UK) and are presented in Fig. 3. Distinct resonances are found at ~15 MHz for all of the transducers as per the design specification, corresponding to the fundamental thickness mode. All the smaller responses away from the main resonance peaks are thought to be a result of the transducer housing or fabrication process as these were not observed while characterising the active elements prior to assembly. The electromechanical coupling factors, k_t, calculated from the impedance curves for Trdx-FF1, Trdx-SF1, Trdx-FF2 and Trdx-SF2 are 0.55, 0.53, 0.68, and 0.62, respectively. Higher k_t values are obtained from the composite transducers as expected, demonstrating the advantage of the composite material in improving energy transduction efficiency compared with the monolithic PZT.

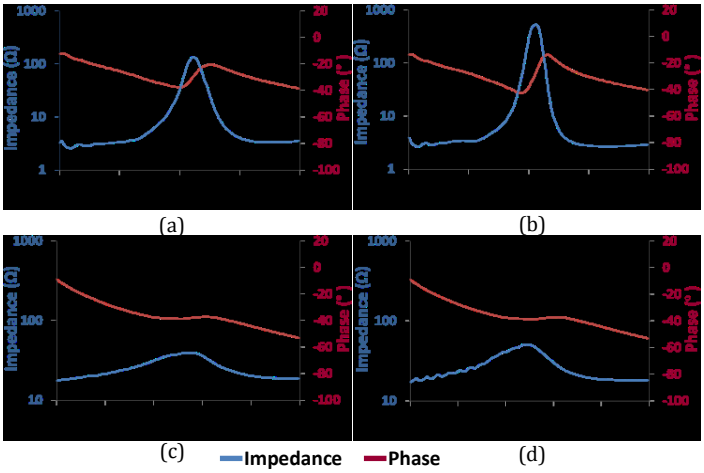

Fig. 3. Impedance and phase diagrams of (a) Trdx-FF1, (b) Trdx-SF1, (c) Trdx-FF2 and Trdx-SF2 needle transducers.

B. Pulse-echo tests

The pulse-echo responses of the transducers were tested using a high frequency pulser-receiver (DPR 500, JSR Ultrasonics, Pittsford, NY, USA). A flat, 1 mm thick glass plate submerged in water was used as the echo target during these measurements. As shown in Fig. 4, the obtained pulse-echo responses present similar central frequency values of ~15–16 MHz for all of the needle transducers, but give significantly broader -6 dB bandwidth values for the composite transducers at 85.7% and 73.7% for the Trdx-FF2 and Trdx-SF2, respectively compared to those of the PZT transducers, which were 19.2% and 13.6% for the Trdx-FF1 and Trdx-SF1, respectively. The -20 dB pulse lengths of four transducers are 1.1 µs, 1.4 µs, 0.14 µs and 0.12 µs.

In the set of transducers incorporating the same active element material with the same dimensions, the one facing sideways showed narrower bandwidth than the one facing forwards. This is probably related to the fact that the thickness of the backing was physically limited to less than 1 mm in the sideways facing Trdx-SF1 and Trdx-SF2 transducers due to small needle diameter, whereas the backing in forward-facing devices was around 5 mm thick. A possible solution may be to increase the bandwidth in the sideways-facing transducers by introducing more damping by increasing the tungsten volume fraction in the backing material.

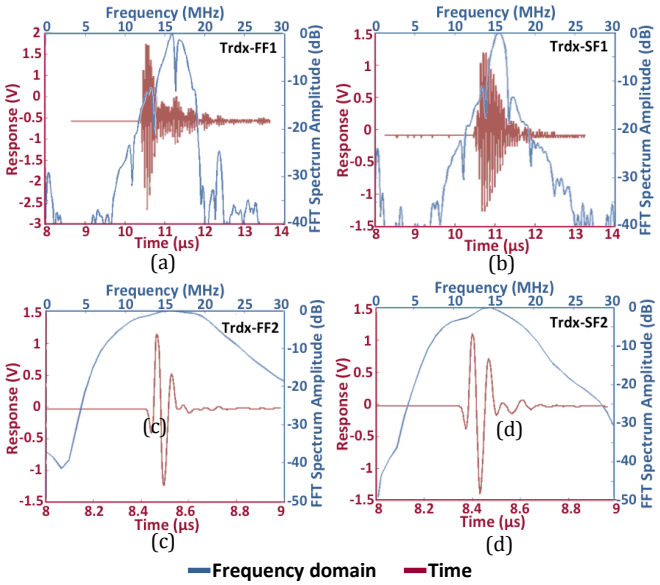

Fig. 4. Pulse-echo response and spectra of (a) Trdx-FF1, (B) Trdx-SF1, (c) Trdx-FF2 and (d) Trdx-SF2 needle transducers.

C. Wire phantom scan

The imaging capabilities of the needle transducers were studied by scanning wire phantoms. The transducers were connected to a scanning system built in-house, programed under LabVIEW (National Instruments, Newbury, UK) environment. For both the forward and side–facing transducers, the needles were attached to an automatic linear scanning stage controlled by a SHOT-602 stage controller (Sigma Koki, Tokyo, Japan), and the reflected echo through the pulser-receiver was captured and saved with an oscilloscope (MDO3024, Tektronix, Oregon, United States) for post image processing. Two wire phantoms were prepared

in order to carry out the characterisation. For the forward-facing transducers, the phantom was made of eight tungsten wires of 20 µm in diameter, positioned in a bespoke holder so that they were separated by 1 mm along the axial and lateral directions. For the side-facing transducers, a radial wire phantom was made of a rapid prototyped holder and six nylon fishing wires of 0.7 mm diameter, which were positioned at various radial distances within the holder. Linear scans were performed with the forward-facing transducer moving step by step over the tungsten wire phantom. For scanning using the side-facing transducers, the system configuration is similar but the needle transducers remained in a fixed central position whilst the radial fishing wire phantom was rotated on a motorized precision rotation stage (PRM1Z8 mount with TDC001 T-Cube DC Servo Motor Controller, Thorlab, New Jersey, USA). All scanning were carried out with transducers and wire phantoms submerged in water.

The linear scan and rotating images are displayed with the dynamic range of 35 dB and 40 dB respectively, as shown in Fig. 5. Both images produced by the composite transducers have relatively good resolution and low noise, while the images from the PZT transducers are generally noisier. Although, by comparing Fig. 5(c) and (d), the Trdx-SF1 shows higher sensitivity than Trdx-SF2, Trdx-SF1 suffers from a severe "ringing-down" problem in its near field region making it difficult to detect any close targets.

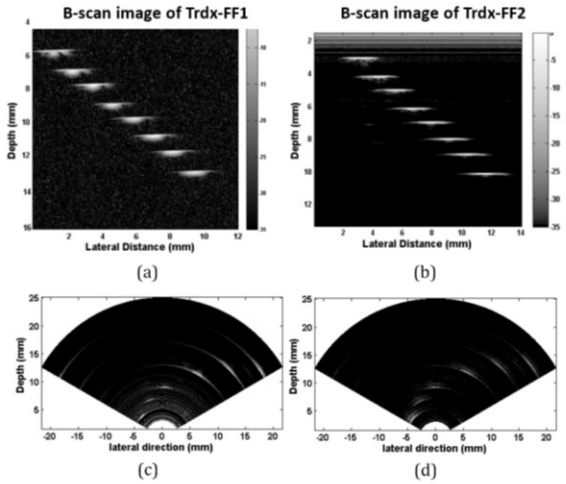

Fig. 5. B-scan images of tungsten wires by (a) Trdx-FF1 and (b) Trdx-FF2 and rotating fish wire scan images by (c) Trdx-SF1 and (d) Trdx-SF2.

IV. Conclusion and Future Work

15 MHz single element needle transducers designed for intraoperative image-guided neurosurgery have been fabricated using commercial PZT bulk ceramic and micro-moulded 1-3 piezocomposites. Various techniques have been developed for the fabrication of the transducers looking forwards and sideways. The impedance and pulse-echo response of these transducers have been characterised and higher coupling, better axis resolution and broader bandwidth have been found for the composite transducers, as expected. The performance of the sideways-facing transducers might be affected by the relatively thin backing and further study on backing material/composition suitable for sideways-facing needle transducer is required. The imaging capabilities of these transducers have also been demonstrated by linear and rotating wire phantom scans. Studies of brain tissue imaging using these transducers will be conducted for further feasibility tests. Based on the experience from these single element transducers, array transducers in a needle will be fabricated in the future.

Acknowledgment

We thank the Engineering and Physical Research Council (EPSRC) in the UK for their financial support through the grant "Ultrasound in a Needle: Minimally-invasive High Resolution Imaging for Neurosurgery" referenced EP/K020250/1.

References

[1] T. M. Peters, "Image-guided surgery: from X-rays to virtual reality," Computer Methods in Biomechanics and Biomedical Engineering, vol. 4, pp. 27-57, 2001.

[2] P. M. Black, T. Moriarty, E. Alexander III, P. Stieg, E. J. Woodard, P. L. Gleason, C. H. Martin, R. Kikinis, R. B. Schwartz, and F. A. Jolesz, "Development and implementation of intraoperative magnetic resonance imaging and its neurosurgical applications," Neurosurgery, vol. 41, pp. 831-845, 1997.

[3] D. L. Hill, C. R. Maurer Jr, R. J. Maciunas, J. A. Barwise, M. J. Fitzpatrick, and M. Y. Wang, "Measurement of intraoperative brain surface deformation under a craniotomy," Neurosurgery, vol. 43, pp. 514-526, 1998.

[4] P. Hastreiter, C. Rezk-Salama, G. Soza, M. Bauer, G. Greiner, R. Fahlbusch, O. Ganslandt, and C. Nimsky, "Strategies for brain shift evaluation," Medical Image Analysis, vol. 8, pp. 447-464, 2004.

[5] M. M. J. Letteboer, P. W. Willems, M. A. Viergever, and W. J. Niessen, "Brain shift estimation in image-guided neurosurgery using 3-D ultrasound," Biomedical Engineering, IEEE Transactions on, vol. 52, pp. 268-276, 2005.

[6] M. P. Sindou, "Practical handbook of neurosurgery", Springer, 2009.

[7] E. Alexander III, T. Moriarty, R. Kikinis, P. Black, and F. Jolesz, "The present and future role of intraoperative MRI in neurosurgical procedures," Stereotactic and functional neurosurgery, vol. 68, pp. 10-17, 1997.

[8] S. Zausinger, C. Schichor, E. Uhl, M. F. Reiser, and J.-C. Tonn, "Intraoperative CT in Neurosurgery," in Intraoperative Imaging and Image-Guided Therapy, ed: Springer, 2014, pp. 529-536.

[9] M. Ivanov, S. Wilkins, I. Poeata, and A. Brodbelt, "Intraoperative ultrasound in neurosurgery – a practical guide," British Journal of Neurosurgery, vol. 24, pp. 510-517, 2010.